

## Responses to Reviewer 1

Provided below are responses to reviewer comments, which are highlighted using bold text.

## Summary

The work "Wavelet analysis for non-stationary, non-linear time series" by J.A. Schulte is devoted to developing methods for wavelet bicoherence estimation with testing for statistical significance and estimating confidence bands. Correspondingly, the author claims five objectives of the work. As illustrative examples, simple mathematical signals are used as well as geophysical data (quasi-biennial oscillation time series). Overall, the manuscript is clearly written. I regard it as quite correct. The field to which the work belongs (special methods for nonlinear characterization of time series taking into account statistical fluctuations of the estimates and controlling statistical significance of the conclusions) is important in geophysics and interesting for a wider physical audience. However, I think that the presented results are not sufficiently original and novel to be published as a separate paper. They make an impression of relevant, but secondary and quite evident technical peculiarities which should be taken into account when applying the wavelet bicoherence estimation technique to real-world data. In my opinion, the author should either (i) show that these peculiarities are not so evident or (despite their evidence) unexpectedly fruitful or (ii) obtain new useful knowledge about realworld data with the aid of the methods considered. Both of these criteria are not met. Moreover, I stress my impression that the author **CONSIDERS** the estimation methods rather than **SUGGESTS** them. Below, I list more concrete and detailed critical remarks considering the objectives claimed in the Introduction one-by-one.

The author is thankful for the detailed comments provided by the reviewers. Both reviewers found the paper to be well-written and without error but felt that it was not original. No substantial changes have been made to the manuscript besides some additional text to better highlight the research undertaken in the use of the new methodologies. While not any one method presented in the manuscript is a significant original contribution, the synthesis of methods together with small improvements of existing methods represents an original contribution to higher-order wavelet analysis. The literature regarding the subject has primarily focused on its theoretical and geophysical applications and to a lesser extent on the statistical

1 aspects of the subject. This paper represents the first synthesis and detailed  
2 discussion of various statistical procedures that should be considered when applying  
3 higher-order wavelet analysis. This paper largely follows the overall structure of the  
4 well-known works of Grinsted (2004) and Torrence and Compo (1998), which  
5 bridged gaps between the signal processing aspects of wavelet analysis and  
6 statistical facets of the subject. Indeed, the manuscript has put higher-order wavelet  
7 analysis in a statistical framework and bridges that same gap as the aforementioned  
8 works. The author has also created the first higher-order wavelet analysis Matlab  
9 software package corresponding to the paper, which will be of importance to a  
10 broader geophysical community.

11 No substantial changes have been made to the manuscript besides some additional  
12 text to better highlight the research undertaken in the use of the new methodologies.

### 13 Specific Points

14 **1) Before other comments, I note that almost the same formalism was already  
15 suggested and applied in several works. In particular, in Ref. [J.Jamsek et al //  
16 PHYSICAL REVIEW E, v. 76, 046221 (2007)] the authors did the same things,  
17 except that they did not estimate statistical significance. The latter was just not  
18 very important for their problems due to the presence of clearly constant  
19 biphase as compared to the periods of varying biphase.**

20 The earlier work of Jamsek et al. (2003) focused on the signal processing  
21 aspects of Fourier-based bispectral analysis. The present manuscript represents an  
22 improvement from that earlier work in that the author has extended the formalism to  
23 wavelet analysis and used statistical hypothesis testing. Also included in the present  
24 manuscript are applications of new methods from traditional wavelet analysis to  
25 higher-order wavelet analysis. To the author's knowledge, no such up-to-date  
26 synthesis currently exists.

27 **2) Page 1709, lines 4-5. "... the first objective of this paper is to develop  
28 significance testing methods for higher-order wavelet analysis to aid physical  
29 interpretation of results".**

30 **In fact, the author just suggests to generate red-noise (AR(1)) surrogates,  
31 estimate wavelet bispectrum from them and compare it with the estimates  
32 obtained from the data at hand. This approach is widely used for many  
33 significance testing problems, e.g. for the wavelet coherence estimation as the  
34 author correctly points out (Jevereyeva et al, 2003; Grinsted et al, 2004). Thus,**

1 the author just reminds us here that it is relevant to perform significance testing  
2 when estimating the wavelet bicoherence too (this is evident but it is good to  
3 remember about it in practice) and suggests to use a well-known approach for  
4 that. Thus, the first objective is achieved before doing any research.

5 While the author agrees that Monte Carlo methods are widely used, their use in  
6 higher-wavelet order analysis has received little attention. The author reminds the  
7 reader of the use of such methods in wavelet analysis before proceeding to more  
8 specialized topics later in the manuscript. However, the author agrees that this part  
9 of the paper should be not be listed as an objective and therefore the text on Page  
10 1709 Line 4 has been deleted.

11 **3) Page 1709, lines 9-10. "... second objective of this paper will be therefore to  
12 apply statistical methods controlling false positive detection."**

13 **This is also correct that multiple testing should be taken into account. This is  
14 relevant here since many values of the wavelet bispectrum are estimated. It is  
15 well-known that Bonferroni correction or a bit elaborated Benjamini  
16 corrections can be applied. The author just suggests to apply these techniques  
17 during the wavelet bicoherence estimation (namely, he prefers Benjamini FDR  
18 controlling scheme). No modification of the techniques is needed. Thus, the  
19 second objective is also achieved before doing any research.**

20 Controlling false positive detection represents an important and long-  
21 established topic in statistics. Yet, its necessity in wavelet analysis was only first  
22 realized years after the influential work of Torrence and Compo (1998) by Maraun  
23 and Kurths (2004) and later by Maraun et al. (2007), Schulte et al. (2015), and  
24 Schulte (2016). The inclusion of the Benjamini scheme in the manuscript represents  
25 an original contribution in that it bridges the gap between higher-order wavelet  
26 analysis and statistical hypothesis testing.

27 **4) Page 1709, lines 11-14. "The third objective of this paper will be to develop  
28 a procedure for calculating confidence intervals corresponding to the sample  
29 estimates, which represent a range of plausible values for the sample  
30 estimates".**

31 **Here, the authors suggests to use a bootstrapping technique with replacement.  
32 Taking into account autocorrelations of subsequent wavelet coefficients, it  
33 becomes block bootstrapping. It is Ok, but also well-known. Thus, again the  
34 authors suggests to use previously known approach.**

1 The author respectfully disagrees that the bootstrapping method is not novel.  
2 To the author's knowledge, confidence interval estimation using the block  
3 bootstrapping method has never been applied to autobicoherence spectra. While the  
4 method is well known, its application in wavelet analysis is not straightforward. The  
5 difficulty of its application arises because the calculation of the autobicoherence  
6 spectrum uses wavelet coefficients at the three wavelet scales and the correlation  
7 structure of the wavelet coefficients differs at each of the scales. Therefore, a Monte  
8 Carlo simulation was conducted to carefully determine the appropriate block length  
9 needed to accurately estimate confidence intervals. In the Monte Carlo simulation,  
10 autobiocherence spectra of red-noise processes were calculated and the 95%  
11 confidence intervals of the autobicoherence estimates were calculated. The width of  
12 the confidence interval was computed at each to scale to determine when the  
13 confidence interval widths generally are the widest. The block length at which  
14 confidence intervals were generally the widest was determined to be the best  
15 estimate of the appropriate block length. The Monte Carlo analysis was a lengthy  
16 process that required some research. Details of the procedure are now included in  
17 the manuscript and are inserted on Page 1723 Line 5.

18 **5) Page 1709, lines 18-20. "Objective four of this paper will address the time  
19 interval selection problem. Such an approach has already been adopted in  
20 wavelet coherence analysis (Grinsted et al., 2004)."**

21 **Again, everything is correct and relevant, but the technique was suggested  
22 before for the cross-wavelet analysis. Here, the author just uses it for the  
23 wavelet bicoherence analysis. No special research is needed here and no spesial  
24 research is in fact performed by the autors concerning this point.**

25 The use of the smoothing operator to calculate local biphase and  
26 autobicoherence represents an improvement from the earlier work of Jamsek (2003)  
27 where the less efficient Fourier analysis was used. Moreover, its use links the earlier  
28 work of Grinsted (2004) with that of Jamsek et al. (2003), representing an original  
29 contribution in higher-order wavelet analysis. A researcher of higher-order wavelet  
30 analysis unaware of the work by Grinsted et al. (2004) would find the use of the  
31 smoothing operator in this work not so evident, again highlighting the importance of  
32 synthesis. The application of the smoothing operator to autobiocherence required  
33 some care because autobicoherence is calculated using wavelet coefficients at three  
34 different scales. Research was needed to determine precisely how the smoothing  
35 operators should be applied. Additionally, statistical significance of the local

1      autobicoherence was addressed in this paper, which was not considered by Jamsek  
2      et al. (2003), again representing an original contribution to the field. The theoretical  
3      example used in this paper demonstrates the use of the local autobicoherence  
4      spectrum and shows how it can measure non-stationary non-linear behavior.

5      **6) Page 1709, line 25. "objective five of this paper will be to introduce a local**  
6      **biphase spectrum".**

7      **Time-varying biphase spectrum was already considered e.g. in Ref. [J. Jamsek,**  
8      **A. Stefanovska, P. V. E. McClintock, and I. A. Khovanov, Phys. Rev. E 68,**  
9      **016201 (2003)] where the authors used short-time Fourier transform. Thus, the**  
10     **idea itslef was already applied and the properties of the biphase were discussed**  
11     **with several examples. Here, the author implements the idea with wavelets but**  
12     **the modificati Time-varying biphase spectrum was already considered e.g. in**  
13     **Ref. [J. Jamsek, A. Stefanovska, P. V. E. McClintock, and I. A. Khovanov, Phys.**  
14     **Rev. E 68, 016201 (2003)] where the authors used short-time Fourier transform.**  
15     **Thus, the idea itslef was already applied and the properties of the biphase were**  
16     **discussed with several examples. Here, the author implements the idea with**  
17     **wavelets but the modification is quite obvious (even if it was not applied before).**  
18     **Probably, the author can insist here on that the adaptive smoothing with**  
19     **operators S\_scale and S\_time used by him (following the work of Grinsted et**  
20     **al, 2004) are very fruitful and make the method especially efficient. However,**  
21     **no investigations of this point are described. The author just describes the idea**  
22     **(quite correct and relevant, but quite evident) and does not show that it gives**  
23     **unexpected (in any way) or especially useful results. on is quite obvious (even if**  
24     **it was not applied before). Probably, the author can insist here on that the**  
25     **adaptive smoothing with operators S\_scale and S\_time used by him (following**  
26     **the work of Grinsted et al, 2004) are very fruitful and make the method**  
27     **especially efficient. However, no investigations of this point are described. The**  
28     **author just describes the idea (quite correct and relevant, but quite evident)**  
29     **and does not show that it gives unexpected (in any way) or especially useful**  
30     **results.**

31     Please see response to comment 5.

32     **7) The author illustrate the technique with QBO time series. However, the**  
33     **conclusions made are that the time series under study is skewed (negative**  
34     **phases are stronger than positive) and asymmetric (transition from easterlies**  
35     **to westerlies is more rapid than the opposite one). However, this can be seen by**

1 eye directly from the time series as he author states himself. Thus, it is not clear  
2 what an especially useful knowledge is given by the suggested technique. That  
3 the technique works as expected is not a new knowledge.

4 The application of higher-order wavelet analysis to QBO time series alone  
5 represents an original contribution in that it has never been applied to it. The purpose  
6 of using this geophysical example was that nonlinearities in the time series are  
7 readily visible, allowing the reader to better connect the methods to a real-world  
8 example. This physical example is an important bench mark for future uses of the  
9 methods.

10 **8) Throughout the paper, the author often uses such term as "interaction of the**  
11 **components". E.g. page 1718, lines 22-24: "The power at lambda = 14 months**  
12 **therefore partially resulted from the interaction between its primary frequency**  
13 **component and its harmonic". It is not clear what "interaction" is implied here.**  
14 **The use of such a term seems quite vague. I agree that there is a statistical**  
15 **dependency between the phases of the two spectral components. In particular,**  
16 **it can be a result of a static quadratic nonlinearity of the "system under study",**  
17 **i.e. possibly there is a signal with the period of 28 months at the input of "the**  
18 **system under study", then the signal is squared so that the second harmonic is**  
19 **generated. In this simple picture, no interaction takes place and no separate**  
20 **interacting modes are present. Certainly, other interpretations can be imagined.**  
21 **However, constancy of the biphase cannot be per se an unequivocal sign of**  
22 **"interaction" between something and something.**

23 The author largely agrees with the assessment. The word "interaction" we  
24 be replaced by "statistical dependence" or "statistically dependent" where  
25 appropriate.

26

27

28

29

30

31

1    **References**

2    Grinsted, A., Moore, J. C., and Jevrejeva, S.: Application of the cross wavelet  
3    transform and wavelet coherence to geophysical time series, *Nonlin. Processes  
4    Geophys.*, 11, 561-566, doi:10.5194/npg-11-561-2004, 2004.

5    J. Jamsek, A. Stefanovska, P. V. E. McClintock, and I. A. Khovanov, *Phys. Rev. E*  
6    68, 016201 (2003)

7    Maraun, D. and Kurths, J.: Cross wavelet analysis: significance testing and pitfalls,  
8    *Nonlin. Processes Geophys.*, 11, 505-514, 2004. 31

9

10    Maraun, D., Kurths, J., and Holschneider, M.: Nonstationary Gaussian processes in  
11    wavelet domain: synthesis, estimation, and significance testing, *Phys. Rev. E*, 75,  
12    doi: 33 10.1103/PhysRevE.75.016707, 2007.

13    Torrence, C. and Compo, G. P.: A practical guide to wavelet analysis, *Bull. Amer.  
14    Meteor. Soc.*, 8 79, 61–78, 1998.

15    Schulte, J. A., Duffy, C., and Najjar, R. G.: Geometric and topological approaches  
16    to significance testing in wavelet analysis, *Nonlin. Processes Geophys.*, 22, 139-  
17    156, 2015.

18    Schulte, J. A.: Cumulative areawise testing in wavelet analysis and its application to  
19    geophysical time series, *Nonlin. Processes Geophys.*, 23, 45-57, doi:10.5194/npg-  
20    23-45-2016, 2016.

21    **Responses to Reviewer 2**

22    Provided below are responses to reviewer comments, which are highlighted using  
23    bold text.

24    **Summary**

25    **This paper considers the problem of detecting and quantifying nonlinearities in  
26    nonstationary time series with wavelet-based approaches. The author aims to  
27    study abilities of the higher-order wavelet analysis in application to the Quasi-  
28    biennial Oscillation time series. He considers five objectives, namely, to develop  
29    significance testing methods for higher-order wavelet analysis, to apply statistical  
30    methods controlling false positive detection, to develop a procedure for  
31    calculating confidence intervals corresponding to the sample estimates, to solve**

1 the problem of selection of a time interval for calculations, and to introduce a  
2 local biphase spectrum.

3 The paper is well written and contains a clear description of approaches for  
4 wavelet bicoherence estimation that could be interesting for researchers dealing  
5 with nonstationary and nonlinear time series. In my opinion, the description of  
6 the methods and their geophysical applications can be used as a part of a review  
7 paper or a monograph devoted to the higher-order wavelet analysis. However, I  
8 have doubts concerning publishing this manuscript as a research paper. Actually,  
9 earlier known approaches are applied to simple testing signals and geophysical  
10 data, and the originality and the novelty of the discussed approaches and the  
11 obtained results is unclear.

12 The author is thankful for the detailed comments provided by the reviewers. Both  
13 reviewers found the paper to be well-written and without error but felt that it was  
14 not original. No substantial changes have been made to the manuscript besides some  
15 additional text to better highlight the research undertaken in the use of the new  
16 methodologies. While not any one method presented in the manuscript is a  
17 significant original contribution, the synthesis of methods together with small  
18 improvements of existing methods represents an original contribution to higher-  
19 order wavelet analysis. The literature regarding the subject has primarily focused on  
20 its theoretical and geophysical applications and to a lesser extent on the statistical  
21 aspects of the subject. This paper represents the first synthesis and detailed  
22 discussion of various statistical procedures that should be considered when applying  
23 higher-order wavelet analysis. This paper largely follows the overall structure of the  
24 well-known works of Grinsted (2004) and Torrence and Compo (1998), which  
25 bridged gaps between the signal processing aspects of wavelet analysis and  
26 statistical facets of the subject. Indeed, the manuscript has put higher-order wavelet  
27 analysis in a statistical framework and bridges that same gap as the aforementioned  
28 works. The author has also created the first higher-order wavelet analysis Matlab  
29 software package corresponding to the paper, which will be of importance to a  
30 broader geophysical community.

31 No substantial changes have been made to the manuscript besides some additional  
32 text to better highlight the research undertaken in the use of the new methodologies.

33 **Specific Points**

1 Thus, in particular, the significance testing method used the author has only  
2 minor distinctions from those discussed in other papers (e.g., Grinsted et al,  
3 2004). Also, I did not find novelty in the used statistical methods controlling  
4 false positive detection and in calculating confidence intervals corresponding to  
5 the sample estimates. The author did a good work in application of known  
6 techniques and their description with pointing out many important things,  
7 however, the claimed objectives are different from the presented results. In  
8 conclusion, I think that the considered topic may be interesting for a broad  
9 physical community, but I do not recommend publication of this work in its  
10 present form.

11 Please see responses to comments 2 through 5 of Reviewer 1

12

13 **Wavelet Analysis for Non-stationary, Non-linear Time Series**

14 **Justin A. Schulte**

15 **The Pennsylvania State University, University Park,  
16 Pennsylvania 16802**

17 **Abstract**

18 Methods for detecting and quantifying nonlinearities in nonstationary time series are introduced  
19 and developed. In particular, higher-order wavelet analysis was applied to an ideal time series and  
20 the Quasi-biennial Oscillation (QBO) time series. Multiple-testing problems inherent in wavelet  
21 analysis were addressed by controlling the false discovery rate. A new local autocohherence  
22 spectrum facilitated the detection of local nonlinearities and the quantification of cycle geometry.  
23 The local autocohherence spectrum of the QBO time series showed that the QBO time series  
24 contained a mode with a period of 28 months that was phase-coupled to a harmonic with a period  
25 of 14 months. An additional nonlinearly interacting triad was found among modes with periods of  
26 10, 16, 26 months. Local biphase spectra determined that the nonlinear interactions were not  
27 quadratic and that the effect of the nonlinearities was to produce non-smoothly varying  
28 oscillations. The oscillations were found to be skewed so that negative QBO regimes were

1 preferred, and also asymmetric in the sense that phase transitions between the easterly and westerly  
2 phases occurred more rapidly than those from westerly to easterly regimes.

3 **1. Introduction**

4 Spectral analysis is a tool for extracting embedded structures in a time series. In particular,  
5 Fourier analysis has been used extensively by researchers for extracting deterministic structures  
6 from time series but is incapable of detecting nonstationary features often present in geophysical  
7 time series. Wavelet analysis can extract transient features embedded in time series, with a wavelet  
8 power spectrum representing variance (power) of a time series as a function of time and period.  
9 Since the seminal work of Torrence and Compo (1998), wavelet analysis has been applied  
10 extensively to geophysical time series such as the indices for the North Atlantic Oscillation (Olsen  
11 et al., 2012), Arctic Oscillation (Jevrejeva et al., 2003), Pacific Decadal Oscillation (Macdonald  
12 and Case, 2005; Newmann et al., 2003), El-Niño/Southern Oscillation (ENSO; Torrence and  
13 Webster, 1999), Pacific-North American Pattern, and West Pacific pattern (Gan et al., 2007). The  
14 application of wavelet coherence and cross-wavelet analyses (Grinsted et al., 2004), moreover, has  
15 proven useful in relating geophysical time series to other time series (Jevrejeva et al., 2003; Gan  
16 et al., 2007; Labat, 2010; Lee and Lwiza, 2008).

17 Many statistical methods, including power and cross-spectral analyses, rely on the assumption  
18 that the variable in question is Gaussian distributed (King, 1996). For a linear system in which the  
19 output is proportional to the input, the first- and second-order moments, the mean and variance,  
20 can fully describe the distribution of a process. In the frequency domain, by analogy, the variable  
21 can be fully described by the power spectrum, the decomposition of variance as a function of  
22 frequency. Suppose, however, that the distribution is non-Gaussian so that higher-order moments  
23 such as skewness and kurtosis exist. In this case, the mean and variance, while useful, are unable  
24 to fully describe the distribution in question. In a time series context, non-Gaussian distributions  
25 can arise from nonlinear systems, systems for which the output is no longer simply proportional  
26 to the input. For a nonlinear system, if the input is the sum of two sinusoids with different  
27 frequency components the output will contain additional frequency components representing the  
28 sum and difference of the input frequencies (King, 1996). In such cases, it is necessary to examine  
29 the decomposition of higher-order moments in frequency space.

1 The frequency decomposition of the third-order moment, for example, results in a bispectrum  
2 or skewness function that measure deviations from Gaussianity (Nikias and Raghubeer, 1987;  
3 King, 1996). In fact, Hinich (1985) developed a bispectral test to determine if a time series is non-  
4 Gaussian and nonlinear. In some situations, higher-order nonlinearities such as cubic nonlinearities  
5 may exist, in which case the trispectrum or other polyspectra would have to be used (Collis et al.,  
6 1998).

7 Another advantage of higher-order spectral analysis is that the cycle geometry of oscillations,  
8 such as asymmetry with respect to a horizontal axis (skewed oscillation) or with respect to a  
9 vertical axis (asymmetric oscillation) can be quantified using the biphase. A pure sine wave, for  
10 example, is neither skewed nor asymmetric, whereas a time series resembling a saw-tooth is  
11 asymmetric. Skewed and asymmetric cycle geometry can identify, for example, abrupt climatic  
12 shifts, sudden shifts in the climate system that exceed the magnitude of the background variability  
13 (King, 1996). Abrupt climate shifts have occurred numerous times in the past and have dire  
14 impacts on ecological and economic systems (Alley et al., 2005). An understanding of past abrupt  
15 climate shifts is essential to understanding future climate change and so there is a need to quantify  
16 nonlinearities present in climatic oscillations.

17 The Quasi-biennial Oscillation (QBO), as another example, has been shown to behave  
18 nonlinearly, transitioning from easterly phases to westerly phases more rapidly than from westerly  
19 to easterly phases (Lu et al., 2009). Another source of asymmetry in the QBO time series arises  
20 from the westerly shear zone descending more regularly than the easterly shear zone. Asymmetries  
21 in the QBO time series are not well-captured by linear methods such as linear principal component  
22 and singular spectrum analyses (Lu et al., 2009) but are better captured using, for example,  
23 nonlinear principal component analysis (Hamilton and Hsieh, 2002). Another example of a  
24 nonlinear time series is the sunspot cycle. Solar activity undergoes an 11-year oscillation  
25 characterized by asymmetric cycle geometry, with solar maxima generally rising faster than they  
26 fall, indicating the presence of nonlinearities (Moussas et al., 2005; Rusu, 2007). ENSO, a climate  
27 phenomenon with regional- to global-scale impacts, has also been shown to exhibit nonlinearities  
28 (Timmermann, 2003). The presence of nonlinearities and possible nonstationarities in the QBO,  
29 ENSO, and sunspot time series makes traditional Fourier and wavelet analysis inadequate for

1 feature extraction, underscoring the need to develop methods for quantifying nonlinearities in a  
2 nonstationary geophysical setting.

3 The application of higher-order wavelet analysis has been rather limited compared to  
4 traditional wavelet analysis (van Milligan et al., 1995; Elsayed, 2006). One geophysical  
5 application of higher-order wavelet analysis is to oceanic waves (Elsayed, 2006), which was found  
6 to be capable of identifying nonlinearities in wind-wave interactions. However, the study lacked  
7 rigorous statistical significance testing, which is problematic because even a Gaussian process of  
8 finite length can produce nonzero bicoherence. Therefore, the first aspect objective of this paper  
9 is to apply develop significance testing methods for higher-order wavelet analysis to aid physical  
10 interpretation of results.

11 The number of bicoherence estimates to which the statistical test is applied will be large and  
12 multiple artifacts will result. The multiple-testing problem was already identified for traditional  
13 wavelet analysis (Maraun et al., 2007; Schulte et al., 2015, Schulte, 2016). The first second  
14 objective of this paper will be therefore to apply statistical methods controlling false positive  
15 detection. It is also noted that the bicoherence spectra calculated are only sample estimates of the  
16 true bicoherence spectra. The second third objective of this paper will be to develop a procedure  
17 for calculating confidence intervals corresponding to the sample estimates, which represent a range  
18 of plausible values for the sample estimates.

19 Another problem with the application of higher-order wavelet analysis is selection of a time  
20 interval on which to calculate the high-order wavelet quantities. Such an approach is subjective  
21 and the result of the analysis may depend on the time interval chosen. Objective three four of this  
22 paper will address the time interval selection problem. Such an approach has already been adopted  
23 in wavelet coherence analysis (Grinsted et al., 2004).

24 Additionally, properties of the biphase have only been examined for Fourier-based bispectral  
25 analysis (Elgar and Sebert, 1989; Maccarone, 2013) and its usefulness in higher-order wavelet  
26 analysis has yet to be examined. For nonstationary time series, the biphase and cycle geometry  
27 corresponding to the time series may change with time and thus objective four five of this paper  
28 will be to introduce a local wavelet-based biphase spectrum.

1 In this paper, higher-order wavelet analysis is put in a statistical framework and applied to the  
 2 QBO time series to demonstrate the insights afforded by the methods. Before describing higher-  
 3 wavelet analysis, a brief overview of wavelet analysis is first presented in Sect. 2. Higher-order  
 4 wavelet analysis is described in Sect. 3 and a new local autocohherence spectrum is introduced,  
 5 eliminating the selection of a time interval on which to calculate nonlinear properties of time series.  
 6 The new and existing methods are applied to an ideal time series and the QBO index. In Section  
 7 4, a new procedure for estimating confidence intervals of global autocohherence quantities is  
 8 developed to estimate uncertainties in the sample autocohherence spectra. The application of the  
 9 new procedure to the sample autocohherence spectrum of the QBO time series is then used to  
 10 further assess confidence in results.

## 11 2. Wavelet Analysis

12 The idea behind wavelet analysis is to convolve a time series with a function satisfying certain  
 13 conditions. Such functions are called wavelets, of which the most widely used is the Morlet  
 14 wavelet, a sinusoid damped by a Gaussian envelope:

$$15 \quad \psi_0(\eta) = \pi^{-1/4} e^{i\omega_0\eta} e^{-\frac{1}{2}\eta^2}, \quad (1)$$

16 where  $\psi_0$  is the Morlet wavelet,  $\omega_0$  is the dimensionless frequency, and  $\eta$  is the dimensionless  
 17 time (Torrence and Compo, 1998; Grinsted et al., 2004). In practical applications, the convolution  
 18 of the wavelet function with a time series  $X = (x_n; n = 1, \dots, N)$  is calculated discretely using

$$19 \quad W_n^X(s) = \sqrt{\frac{\delta t}{s}} \sum_{n'=1}^N x_{n'} \psi_0[(n' - n) \frac{\delta t}{s}], \quad (2)$$

20 where  $\delta t$  is a uniform time step,  $s$  is scale,  $\eta = s \cdot t$ , and  $W_n^X(s)$  is the wavelet transform. The  
 21 wavelet power is given by  $|W_n^X(s)|^2$  (Torrence and Compo, 1998; Grinsted et al., 2004). For the  
 22 Morlet wavelet with  $\omega_0 = 6$ , the wavelet scale and the Fourier period  $\lambda$  are approximately equal  
 23 ( $\lambda = 1.03s$ ). A more detailed discussion of wavelet analysis can be found in Torrence and Compo  
 24 (1998).

25 Shown in Fig. 1a is the time series of the QBO index and shown in Fig. 1b is the  
 26 corresponding wavelet power spectrum. The QBO data from 1950-2013 were obtained from the  
 27 Climate Prediction Center. The QBO index is defined as the zonal average of the 30 hPa zonal

1 wind at the equator. As such, a positive index indicates westerly winds and a negative index  
2 indicates easterly winds. The most salient feature of the time series is the rather regular periodicity  
3 of approximately 28 months. Also note the asymmetry between the negative and positive phase,  
4 with the negative phases generally being stronger. The periodic behavior of the QBO was  
5 corroborated by examining the wavelet power spectrum. A well-defined 28-month periodicity is  
6 evident, with the associated wavelet power changing little throughout the study period.

7 There are also secondary features located at a period of approximately 14 months, primarily  
8 from 1985 to 2013. The appearance of significant power at a period of 14 months also coincides  
9 with most of the largest negative phases of the QBO. Such a correspondence may not have been a  
10 coincidence; the 14-month mode and the 28-month mode may have interacted constructively to  
11 generate large negative events but interacted destructively to create smaller positive events.  
12 However, additional tools are needed to confirm if the periodicities are interacting and to  
13 understand how the interactions were related to the behavior of the QBO.

### 14 **3. Higher-order Wavelet Analysis**

#### 15 **3.1 Wavelet-based Autobicoherence**

16 Higher-order spectral analysis provides the opportunity to quantify nonlinearities and allows  
17 the detection of interacting oscillatory modes within a time series. More specifically, nonlinearities  
18 are quantified using bicoherence, a tool for measuring quadratic nonlinearities, where quadratic  
19 nonlinearities imply that for frequencies  $f_1$ ,  $f_2$ , and  $f_3$  and corresponding phases  $\phi_1$ ,  $\phi_2$ , and  $\phi_3$   
20 the sum rules

$$21 \quad f_1 + f_2 = f_3 \quad (3)$$

22 and

$$23 \quad \phi_1 + \phi_2 = \phi_3 \quad (4)$$

24 are satisfied. Whereas Eq. (3) implies frequency coupling, Eq. (4) implies phase coupling. To see  
25 from where Eqs. (3) and (4) originate, let

$$26 \quad X(t) = \sin(2\pi f_1 t + \phi_1) + \sin(2\pi f_2 t + \phi_2) \quad (5)$$

27 be the input into a system whose output is related to the input by

$$Y(t) = X(t) + \varepsilon X(t)^2 + w(t). \quad (6)$$

2 The multiplicative factor  $\varepsilon$  is used to represent the contribution of the nonlinear component of the  
 3 signal and  $w(t)$  is Gaussian white noise. Note that if  $\varepsilon = 0$ , then the system is linear because the  
 4 output contains the same frequency components as the input. The substitution of Eq. (5) into Eq.  
 5 (6) results in

$$\begin{aligned}
Y(t) = & \sin(2\pi f_1 t + \phi_1) + \sin(2\pi f_2 t + \phi_2) + \frac{\varepsilon}{2}[1 - \cos(2(2\pi f_1 t + \phi_1)) \\
& - \cos(2(2\pi f_2 t + \phi_2)) + \cos(2\pi(f_2 - f_1)t + \phi_2 - \phi_1) \\
& - \cos(2\pi(f_1 + f_2)t + \phi_1 + \phi_2)] + w(t) \quad (7)
\end{aligned}$$

9 and thus the output has sinusoids with additional frequency components  $2f_1$ ,  $2f_2$ ,  $f_2 - f_1$ , and  $f_2$   
 10  $+f_1$ , which arise from the second term in right-hand side of Eq. (6).

Unlike the power spectrum, which is the Fourier transform of the second-order moment of a time series, the bispectrum is defined as the double Fourier transform of the third-order moment, or, more generally, the third-order cumulant, i.e.,

$$b_{xxx}(f_1, f_2) = \int_{-\infty}^{\infty} \int_{-\infty}^{\infty} C(t_1, t_2) e^{-i2\pi(f_1 t_1 + f_2 t_2)} dt_1 dt_2, \quad (8)$$

15 where  $C$  is the third-order cumulant, defined as

$$C(t_1, t_2) = M_3(t_1, t_2) + M_1[M_2(t_1) + M_2(t_2) + M_2(t_1 - t_2)] + 2M_1^3 \quad (9)$$

17 and the  $t_i$  are lags. If  $X(t)$  is zero-mean, then in Eq. (9),  $M_1 = E[X(t)] = 0$  denotes the first-order  
 18 moment (mean),  $M_2 = E[X(t)X(t + t_1)]$  denotes the second-order moment (autocorrelation),  
 19 and  $M_3(t_1, t_2) = E[X(t)X(t + t_1)X(t + t_2)]$  denotes the third-order moment (Nidal and Malik,  
 20 2013). Also note that for a zero-mean process, the third-order cumulant reduces to the third-order  
 21 moment (Collis et al., 1998). A more useful quantity is the normalized version of the bispectrum,  
 22 the autocohherence spectrum (Collis et al., 1998), which can be computed using the following:

$$b^2(f_1, f_2) = \frac{|b_{xxx}(f_1, f_2)|^2}{E\left[\left|X_f(f_1)X_f(f_2)\right|^2\right]E\left[X_f(f_1 + f_2)\right]^2}, \quad (10)$$

24 where  $b^2(f_1, f_2)$  is bounded by 0 and 1 by the Schwarz inequality and  $X_f$  denotes the Fourier  
 25 transform of  $X$ .  $b^2(f_1, f_2)$  can be interpreted as the fraction of power at  $f_1 + f_2$  due to quadratic

1 phase coupling among  $f_1$ ,  $f_2$ , and  $f_1 + f_2$  such that the sum rule  $f_1 + f_2 = f_3$  is satisfied (Elgar  
 2 and Chandran, 1993). For a more in-depth discussion of higher-order spectral analysis the reader  
 3 is referred to Nikias and Raghubeer (1987).

4 Phase information and cycle geometry can be obtained from the biphase, which is given  
 5 by

$$6 \quad \psi = \tan^{-1} \left( \frac{\text{Im}(b_{xxx})}{\text{Re}(b_{xxx})} \right) = \phi_1 + \phi_2 - \phi_3. \quad (11)$$

7 It was noted by Maccarone (2013), however, that the biphase should be defined on the full  $2\pi$   
 8 interval and thus in this paper the four-quadrant inverse tangent is computed and not the inverse  
 9 tangent as shown above. By doing so, statistically significant autocohherence detected together  
 10 with the biphase can be used to quantify cycle geometry. A biphase of  $0^\circ$  indicates positive  
 11 skewness and a biphase of  $180^\circ$  indicates negative skewness (Maccarone, 2013). An example of a  
 12 skewed oscillation time series with biphase close to  $0^\circ$  is shown in Fig. 2a. Mathematically, the  
 13 time series is written as

$$14 \quad X(t) = \sum_{j=1}^{40} \frac{1}{j} \cos[0.1jt + a(j-1)], \quad (12)$$

15 where  $a = 0$  (Maccarone, 2013). The time series is skewed because the positive spikes are not  
 16 accompanied by negative spikes of equivalent magnitude and therefore the distribution of the time  
 17 series would be positively skewed, with the right tail being larger than the left tail.

18 For asymmetric waveforms, a biphase of  $90^\circ$  indicates that the time series is linearly rising  
 19 but rapidly falling as shown in Fig. 3, whereas a biphase of  $-90^\circ$  indicates that the time series rises  
 20 rapidly and falls linearly. A purely asymmetric time series will have a biphase of  $90^\circ$  or  $-90^\circ$ , as  
 21 shown in Fig. 3, where the saw-toothed time series obtained by setting  $a = \pi/2$  in Eq. (12) rises  
 22 more slowly than it falls. In a physical setting, asymmetric cycle geometry implies that phase  
 23 transitions occur at different rates, as observed in the QBO time series.

24 According to Elsayed (2006), the wavelet-based autocohherence is defined as

$$25 \quad b_{xxx}^w(s_1, s_2) = \frac{|B_{xxx}^w(s_1, s_2)|^2}{(\int_T |W_x(s_1, t)W_x(s_2, t)|^2 dt)(\int_T |W_x(s, t)|^2 dt)}, \quad (13)$$

26 where

1  $B_{xxx}^W(s_1, s_2) = \int_T W_x^*(s, t) W_x(s_1, t) W_x(s_2, t) dt , \quad (14)$

2  $\frac{1}{s_1} + \frac{1}{s_2} = \frac{1}{s}, \quad (15)$

3

4  $T$  is a time interval,  $W_x(s, t)$  is the wavelet transform of a time series  $X$  at scale  $s$  and time  $t$ , and  
5  $W_x^*(s, t)$  denotes the complex conjugate of  $W_x(s, t)$ . The wavelet-based autocohherence measures  
6 the degree of quadratic phase coupling, where a peak at  $(s_1, s_2)$  indicates an ~~nonlinear interaction~~  
7 ~~statistical dependence among~~ the scale components  $s_1, s_2$ , and  $s$ .

8 In practice, the autocohherence is computed discretely so that Eq. (13) can be written as

9  $\overline{W}_b(s_1, s_2) = \frac{|B_{xxx}^W(s_1, s_2)|^2}{\left(\sum_{n=n_1}^{n_2} |W_n^X(s_1) W_n^X(s_2)|^2\right) \left(\sum_{n=n_1}^{n_2} |W_n^X(s)|^2\right)}, \quad (16)$

10 where

11  $B_{xxx}^W(s_1, s_2) = \sum_{n=n_1}^{n_2} W_n^{*X}(s) W_n^X(s_1) W_n^X(s_2)$   
12  $= \sum_{n=n_1}^{n_2} B_n^W(s_1, s_2), \quad (17)$

13

14  $n_1 \geq 1$ , and  $n_2 \leq N$ . Note that if  $n_1 = 1$  and  $n_2 = N$ , then Eq. (16) represents the global  
15 autocohherence spectrum.

16 The Monte Carlo approach to pointwise significance testing is adopted in this paper and is  
17 similar to that used in wavelet coherence (Grinsted et al., 2014). To estimate the significance of  
18 wavelet-based autocohherence at each point  $(s_1, s_2)$ , Monte Carlo methods are used to (1)  
19 generate a large ensemble of red-noise processes with the same lengths and lag-1 autocorrelation  
20 coefficients as the input time series and (2) compute for each randomly generated red-noise process  
21 the autocohherence spectrum. From the ensemble of autocohherence spectra, the  $p = 100(1 - \alpha_p)$   
22 percentile of the autocohherence estimates is computed for every point  $(s_1, s_2)$ , where  $p$   
23 corresponds to the critical level of the test and  $\alpha_p$  is the pointwise significance level of the test.

1 Given the symmetry of the autocohherence spectrum, the critical level of the test can be computed  
2 using only half of the autocohherence estimates, reducing computational costs.

3 **3.2 Multiple Testing**

4 Let  $\alpha_p$  be the significance level of the pointwise significance test as described above and  
5 let  $K$  denote the number of autocohherence estimates being tested, then there will be on average  
6  $\alpha_p K$  false positive results. A similar problem occurs in traditional wavelet analysis (Maraun et al.,  
7 2007; Schulte et al., 2015; [Schulte, 2016](#)). In the case of simultaneously testing multiple  
8 hypotheses, the number of false positive results can be reduced by applying, for example, the  
9 Bonferroni correction (Lehmann, 1986). However, this simple correction often results in many  
10 true positives being rejected and is especially permissive in the case of autocorrelated data (Maraun  
11 et al., 2004). Other procedures also exist, including the Walker  $p$ -value adjustment procedure,  
12 which has more statistical power than the Bonferroni correction. An even more powerful method  
13 is the Benjamini and Hochberg (1995) procedure, which controls the false discovery rate (FDR),  
14 where the FDR is the expected proportion of the false rejections that are actually true. An  
15 advantage of this method, in addition to its statistical power, is that it takes into account the  
16 confidence with which local hypotheses are rejected and is robust even in the case of autocorrelated  
17 data (Wilks, 2002). Benjamini and Yekutieli (2001) developed a modified version of the Benjamini  
18 and Hochberg (1995) procedure that works for any dependency structure among the local test  
19 statistics and thus this procedure will be used in this paper to control the FDR.

20 The procedure can be described as follows: Suppose that  $K$  local hypotheses were tested.  
21 Let  $p_{(i)}$  denote the smallest of the  $K$  local  $p$ -values, then, under the assumption that the  $K$  local  
22 tests are independent, the FDR can be controlled at the  $q$ -level by rejecting those local tests for  
23 which  $p_{(i)}$  is no greater than

$$24 \quad p_{FDR} = \max_{j=1,\dots,k} [p_{(j)} : p_{(j)} \leq q(j/K)] \\ 25 \quad = \max_{j=1,\dots,k} [p_{(j)} : p_{(j)} \leq \alpha_{global}(j/K)] \quad (18)$$

26 so that the FDR level is equivalent to the global test level. For a local  $p$ -value to be deemed  
27 significant using this procedure, it must be less than or equal to the largest  $p$ -value for which Eq.  
28 (18) is satisfied. If no such local  $p$ -values exist, then none are deemed insignificant, and, therefore,

1 the global test hypothesis cannot be rejected. If the test statistics have an unknown dependency  
2 structure,  $q$  can be replaced with  $q / \sum_{i=1}^K \frac{1}{i}$ , though this substitution makes the procedure less  
3 powerful (Reiner et al., 2002). This modified method will be applied to autocohherence spectra  
4 at the 0.05 level throughout this paper.

5 **3.3 Wavelet-based Autobicoherence of an Idealized Time Series**

6 To demonstrate the features of a time series that can be extracted using higher-order  
7 wavelet analysis, an idealized nonstationary time series will first be considered. Consider the  
8 quadratically nonlinear time series

9 
$$X(t) = \cos(2\pi f t + \phi) + \gamma(t) \cos(4\pi f t + 2\phi) + w(t), \quad (19)$$

10 where  $f$  is frequency,  $w(t)$  is Gaussian white noise, and  $\gamma(t)$  is a time-dependent nonlinear  
11 coefficient given by

12 
$$\gamma(t) = 0.001t. \quad (20)$$

13 Note that Eqs. (3) and (4) are satisfied because  $f_1 + f_2 = 2f_1 = 2f_2$  and similarly for  $\phi$ . The  
14 sinusoid with frequency  $2f_1$  is said to be the harmonic of the primary frequency component with  
15 frequency  $f_2$ , where the amplitude of the harmonic depends on  $\gamma(t)$ , the strength of the quadratic  
16 nonlinearity.  $X(t)$  and the corresponding wavelet power spectrum for the case when  $f_1 = 0.03$  is  
17 shown in Fig. 4. The signal-to-noise ratio of the Gaussian white noise was set to 1 decibels. The  
18 primary frequency component results in a large region of 5% pointwise significance at  $\lambda = 30$ ,  
19 whereas its harmonic only results in a few small significance regions located from  $t = 700$  to  $t =$   
20 1000. It also noted that the appearance of the significance power at  $\lambda = 15$  from  $t = 700$  to  $t =$   
21 1000 is accompanied by large positive spikes in the time series that result in the time series  
22 favoring positive values. Prior to the emergence of the significant power at  $\lambda = 15$ , the time series  
23 varied smoothly in the sense that negative phases were accompanied by positive phases of similar  
24 amplitude.

25 To determine if the oscillations are quadratically interacting, the autocohherence of  $X(t)$   
26 was computed (Fig. 5). The significant peak centered at  $(30, 30)$  indicates that an oscillation with  
27 period 30 is phase-coupled to an oscillation with  $\lambda = 15$ . The result implies that the variability at  
28  $\lambda = 15$  is partially related to the statistical dependence due to the interaction between the two

1 modes. The fraction of variability is determined by the autobicoherence value corresponding to  
 2 the significant peak. In the present case,  $\overline{W}_b(s_1, s_2) = 0.5$  so about half of the variability at  $\lambda =$   
 3 15 is due to the nonlinear interaction. Note that no other peaks were found to be significant.

4 **3.4 Wavelet-based Autobicoherence of Geophysical Time Series**

5 Shown in Fig. 6 is the wavelet-based autobicoherence spectrum for the QBO time series.  
 6 A large region of significance was identified, which contained the local maximum at (28, 28)  
 7 months. The peak represents the phase coupling of the primary frequency component with its  
 8 harmonic with a period of 14 months. The power at  $\lambda = 14$  months therefore is partially related to  
 9 the statistical dependence resulted from the interaction between its primary frequency component  
 10 and its harmonic. The significance and magnitude of the autobicoherence in the QBO spectrum is  
 11 consistent with how the QBO does not vary smoothly, shifting to the easterly phase more quickly  
 12 than to the westerly phase and with the westerly phase tending to be stronger than the easterly  
 13 phase. The asymmetry in both phase transition and magnitude are suggestive of nonlinearities.

14 **3.5 Local Wavelet Autobicoherence**

15 It may also be desirable to see how autobicoherence along slices of the full autobicoherence  
 16 spectrum changes with time. To compute local autobicoherence, apply a smoothing operator  $S(W)$   
 17  $= S_{scale}(S_{time}(W_n^X(s)))$  (Grinsted et al., 2004) to each term in Eq. (13) instead of summing in  
 18 time, i.e.,

$$19 \quad b_n^W(s_1, s_2) = \frac{|S(s_1^{-1}B_n^W(s_1, s_2))|^2}{S(s_1^{-1}|W_n^X(s_1)W_n^X(s_2)|^2) \cdot S(s^{-1}|W_n^X(s)|^2)}. \quad (20)$$

20 The smoothing operator for the Morlet wavelet is given by

$$21 \quad S_{time}(W)|_s = \left( W_n^X(s) * c_1 \frac{-t^2}{2s^2} \right) |_s \quad (21)$$

22 and

$$23 \quad S_{scale}(W)|_n = (W_n^X(s) * c_2 \Pi(.6s))|_n, \quad (22)$$

24 where  $c_1$  and  $c_2$  are normalization constants determined numerically and  $\Pi$  is the rectangular  
 25 function.

1 It is important to mention that the numerator of Eq. (20) contains a term with wavelet  
2 coefficients at two different scales so that the choice of smoothing is not as straightforward as for  
3 wavelet coherence. Smoothing autobicoherence estimates with respect to  $s_{min} = \min(s_1, s_2)$  was  
4 found to result in larger autobicoherence estimates, whereas smoothing the autobicoherence with  
5 respect to  $s_{max} = \max(s_1, s_2)$  resulted in smaller autobicoherence estimates. Given that the  
6 autobicoherence estimates are influenced by the choice of smoothing, it is inevitable that the  
7 significance of the autobicoherence estimates is also impacted. In particular, smoothing the  
8 autobicoherence spectrum with respect to  $s_{max}$  allowed extrema to be smoothed out, eliminating  
9 spuriously large autobicoherence. For this reason, all local autobicoherence spectra in this paper  
10 will be computed by smoothing with respect to  $s_{max}$ .

11 The advantage of using Eq. (20) is that transient quadratic nonlinearities can now be  
12 detected and the need for choosing an integration time interval has been eliminated. If  $s_1 = s_2$ , then  
13  $(t, s_1, s_1) = (t, s_2, s_2) = (t, s)$  and thus, in the case of this diagonal slice, the local wavelet-based  
14 bicoherence spectrum is a two-dimensional representation of the degree of local quadratic  
15 nonlinearity. The vertical axis corresponds to the primary frequency and the horizontal axis  
16 corresponds to time. As a concrete example, a peak at  $(64, 64)$  would indicate that at time index  $t =$   
17 50 the oscillation with a fundamental period  $\lambda = 1.03s \approx 64$  is locally coupled to an oscillation  
18 with period  $\lambda \approx 32$ .

19 One can also compute a local biphase from the smoothed bispectrum by taking the four  
20 quadrant inverse tangent of the smoothed imaginary part divided by the smoothed real part. The  
21 local biphase, for example, was computed for the skewed time series shown in Fig. 2a. As  
22 expected, the biphase fluctuates regularly around  $0^\circ$  and the mean is  $2^\circ$ . The local biphase for the  
23 saw-toothed time series is shown in Fig. 3b. The biphase fluctuates about  $90^\circ$  and the mean biphase  
24 is  $90^\circ$  as expected.

25 The procedure for the estimation of the statistical significance of local autobicoherence is  
26 the following: generate red-noise time series with the same lag-1 autocorrelation coefficients as  
27 the input time series and use the local autobicoherence estimates outside the COI to generate a null  
28 distribution of  $b_n^w(s_1, s_2)$ . Note that the calculation only needs to be performed at a fixed time  
29 outside of the COI because red-noise is a stationary process, which produces a stationary  
30 background spectrum.

1    **3.6 Local Wavelet-based Autobicoherence of an Idealized Time Series**

2       The local autobicoherence spectrum of  $X(t)$  for (30, 30) is shown in Fig. 6b. Initially, there  
3       is no local autobicoherence that exceeds the 5% significance level. At  $t = 250$  and  $t = 500$ , on the  
4       other hand, small regions of 5% significant autobicoherence emerge, indicating a transient  
5       nonlinear interaction. At  $t = 500$  the nonlinearity is strong and results in a large region of significant  
6       local autobicoherence extending from  $t = 500$  to the edge of the wavelet domain

7       In order to determine if the peaks in autobicoherence are associated with a quadratic  
8       nonlinearity, it is important to compute the biphase, which is shown in Fig. 7b. From  $t = 0$  to  $t =$   
9       400 there is an unstable phase relationships between the phase of the primary frequency component  
10      and its harmonic. Such a lack of phase coherence indicates a weak nonlinear interaction, which is  
11      consistent with how the autobicoherence is lower before  $t = 400$ . In contrast, after  $t = 400$ , the  
12      biphase becomes stable, changing little with time, indicating a consistent phase relationship  
13      between the primary frequency mode and its harmonic. It also noted that the biphase during this  
14      time fluctuates near  $0^\circ$ , which implies that the phase relationships arise from a quadratic  
15      nonlinearity. The near zero biphase is consistent with how  $X(t)$  was constructed from the sum of  
16      two cosines with zero phase and also suggests that the interaction results in skewed cycle geometry,  
17      where positive values of the time series are preferred. Indeed, by inspection of Fig. 4a the  
18      oscillations initially appear to be sinusoidal, varying smoothly, whereas after  $t = 400$  spikes begin  
19      to appear and  $X(t)$  favors positive values.

20    **3.7 Local Wavelet-based Autobicoherence of the QBO Time Series**

21       The local autobicoherence spectrum of the QBO index at the point (28, 28) in the full  
22       autobicoherence spectrum is shown in Fig. 8. From 1950 to 1970 the magnitude of the  
23       autobicoherence fluctuated and consisted of one local significant peak at 1965. Significant  
24       autobicoherence was also found from 1975 to 1998, contrasting with the autobicoherence after  
25       1998, which was not found to be significant until 2010.

26       To determine if the peaks indicated in the autobicoherence are associated with a quadratic  
27       nonlinearity, the local biphase was computed. Fig. 8a shows the local biphase for the  
28       autobicoherence peak at (28, 28). For most of the study period, the biphase was found to vary  
29       considerably, particularly during the 1950-1970 and 1995-2013 periods. On the other hand, the

1 biphase varied smoothly from 1970 to 1995, consistent with how the autocohherence during that  
2 period was large and stable (Fig. 8a). Also, during that period the biphase was nonzero; in fact, the  
3 mean biphase during the period was  $-100^\circ$ , suggesting that the phase coupling is not the result of  
4 a quadratic interaction. A biphase of  $-100^\circ$  indicated asymmetric geometry, which physically  
5 represents how phase transitions of the QBO occurred at different rates. Recall that it has already  
6 been discussed in the introduction that the QBO transitions from easterly phases to westerly phases  
7 more rapidly than from westerly to easterly phases (Lu et al., 2009). Another interesting feature is  
8 the general increase in the biphase from 1970 to 1995. In the beginning of the time period, the  
9 biphase was  $-180^\circ$  and after 1980 the biphase switched to  $-90^\circ$ .

10 The local autocohherence and biphase corresponding to the peak (16, 26) was also  
11 computed (Fig. 9). The mean of the absolute value of the biphase for the period 1950-2013 was  
12  $130^\circ$ , indicating a statistical dependency among that the interaction among the modes with periods  
13 of 10, 16, 26 months resulted in skewed waveforms. In fact, because the biphases were close to  
14  $180^\circ$  the waveforms should have been skewed to negative values (Maccarone, 2013) and such  
15 skewness is evident by inspecting Fig. 1. Also note that some of the largest negative phases of the  
16 QBO occurred from 1995 to 2010, which coincided with the period of most significant  
17 autocohherence as shown in Fig. 9a.

## 18 **4. Block Bootstrapping Methods**

### 19 **4.1 Block Bootstrapping Autocohherence**

20 Bootstrapping is a widely used technique to estimate the variance or uncertainty of a  
21 sample estimate. For independent data one samples with replacement individual data points (Efron,  
22 1979); for dependent data one must sample with replacement blocks of data to preserve the  
23 autocorrelation structure of the data (Kunsch, 1989). The latter technique is called block  
24 bootstrapping and should be used for variance estimation of global wavelet quantities, as wavelet  
25 coefficients are known to be autocorrelated in both time and scale. The use of traditional  
26 bootstrapping techniques would result in confidence intervals that are too narrow. It is expected,  
27 however, that the choice of the bootstrapping technique is more critical at larger scales, as the  
28 decorrelation length of the mother wavelet increases with scale.

1 A brief overview of the procedure is provided below but a more detailed discussion can be  
2 found in Schulte et al. (2015). To find the approximate  $100(1 - \beta)\%$  confidence interval of an  
3 autocohherence estimate, divide the set of wavelet coefficients at each scale into overlapping  
4 blocks. The lengths of the blocks at each scale should be the same and the randomly resampled  
5 blocks chosen should be the same at each scale to avoid randomizing the data. The concatenation  
6 of the blocks then results in a synthetic set of wavelet coefficients at each scale. The synthetic set  
7 of wavelet coefficients can then be used to calculate a bootstrap replicate of the autocohherence.  
8 The iteration of the procedure 1000 times results in a distribution of bootstrap replicates from  
9 which a 95% confidence interval can be obtained.

10 As noted by Schulte et al. (2015), the appropriate block length to use can be determined by  
11 Monte Carlo methods. In that study, it was determined from a Monte Carlo experiment that a block  
12 length of  $N^{0.6}$  was found to produce accurate confidence bounds for wavelet coherence while also  
13 producing the widest confidence intervals at all scales. The Monte Carlo experiment was repeated  
14 for 95% confidence in this study because bicoherence estimation requires the use of wavelet  
15 coefficients at three wavelet scales, with the wavelet coefficients at each scale having a different  
16 correlation structure. For wavelet coherence, the block length selection procedure is simpler  
17 because a single wavelet scale is used so that correlaton structure of wavelet coeffients is similiar.  
18 The Monte Carlo experiment was performed by generating red-noise proceses of length 1000  
19 with diffrent lag-1 autocorrelation coefficients and computing 95% confidence intervals around  
20 the estimated autocohherence. Remarkably, the Monte Carlo experiment found that a block length  
21 of  $N^{0.6}$  is also optimal for bicoherence confidence interval estimation. For block lengths exceeding  
22  $N^{0.6}$ , confidence intervals were found to be too narrow, with in some instances the estimated  
23 bicoherence falling outside the 95% confidence interval. It is also noted that the results were  
24 insensitive to the chosen lag-1 autocorrelation coefficient.

#### 25 **4.4.2 Application to Ideal and Climatic Time Series**

26 Figure 5b shows the application of the block bootstrap procedure to the diagonal slice  $s_1 =$   
27  $s_2 = s$  of the autocohherence for the ideal case. The 95% confidence intervals were also obtained  
28 using the ordinary bootstrap. A pronounced peak at  $s = 30$  was identified and represents the  
29 interaction between the primary frequency and its harmonic. By inspection of Fig. 5b, there is a  
30 clear difference between the widths of the confidence intervals obtained from the two

1 bootstrapping procedures. For the ordinary bootstrap, the confidence intervals are narrow and the  
2 widths of the confidence intervals appear to be only weakly dependent on scale. On the other hand,  
3 the confidence intervals obtained using the block bootstrap procedure are wide, especially at large  
4 scales, and the width of the confidence intervals depends strongly on scale, increasing from small  
5 scales to large scales. It is also noted that, whereas the block bootstrap procedure has deemed no  
6 spurious peaks as significant, the ordinary bootstrap procedure deemed two the spurious peaks at  
7  $s = 14$  and  $s = 100$  as significant. The implementation of the block bootstrap procedure can  
8 therefore enhance confidence in results, facilitating the investigation of a deeper physical  
9 understanding.

10 The application of the block bootstrap procedure to the diagonal slice  $s_1 = s_2 = s$  of the  
11 full autocohherence spectrum of the QBO index is shown in Fig 10. The 95% confidence intervals  
12 corresponding to the peaks (14, 14) and (28, 28) do not cross the 5% significance bound and thus  
13 one has more confidence that those peaks are significant. All other peaks have been deemed  
14 insignificant.

15 **5. Summary**

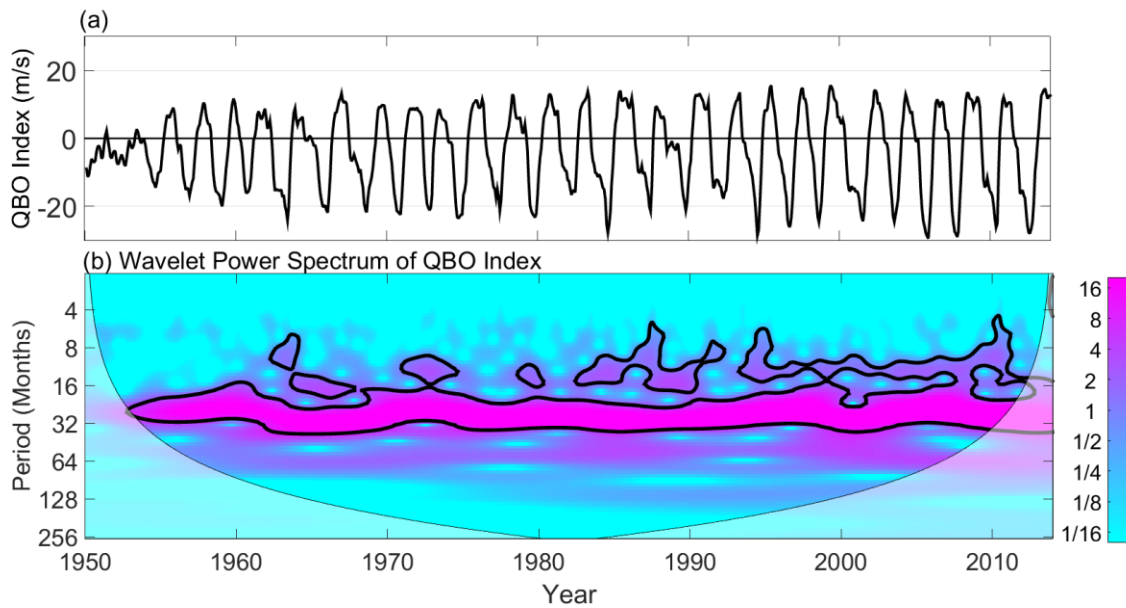
16 Higher-order wavelet analysis together with significance testing procedures were used to  
17 detect nonlinearities embedded in an ideal time series and the QBO time series. The  
18 autocohherence spectrum of the QBO index revealed phase coupling of the 28 month mode with  
19 a higher frequency mode with period 14 months. A local autocohherence spectrum of the QBO  
20 index showed that the strength of the nonlinearities varied temporally. Furthermore, the local  
21 biphase spectrum indicated that a statistical dependence among frequency components the  
22 nonlinear interaction-resulted in waveforms that were both skewed and asymmetric, indicating that  
23 the strength of negative QBO events were stronger than positive events, and that transitions  
24 between events occurred at different rates.

25

1   **Acknowledgements:** Support for this research was provided by the National Science Foundation  
2   Physical Oceanography Program (award number 0961423) and the Hudson River Foundation  
3   (award number GF/02/14).

4

1



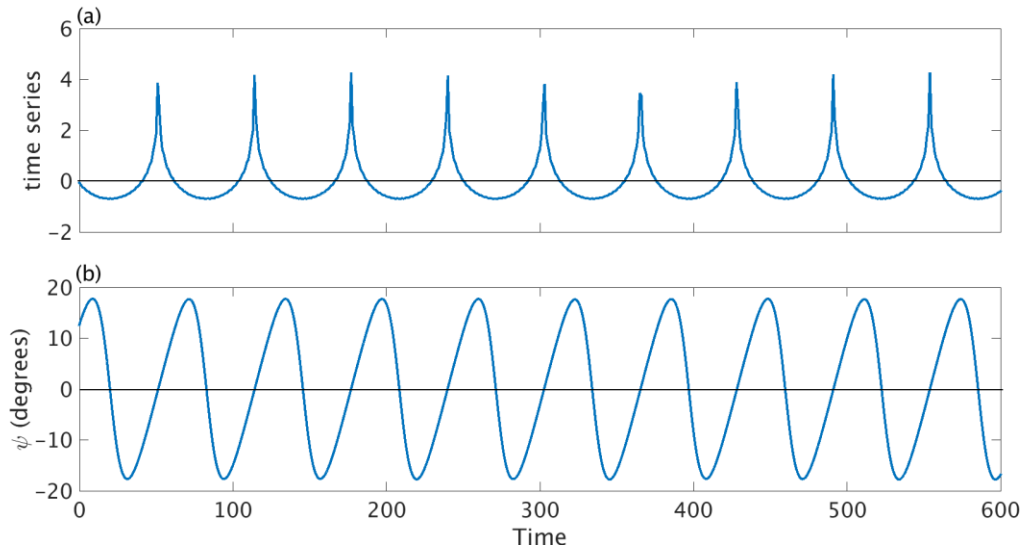
2

3 Figure 1. (a) The QBO index and (b) the corresponding wavelet power spectrum. Contours enclose  
 4 regions of 5% statistical pointwise significance (Torrence and Compo, 1998). Light shading  
 5 represents the cone of influence, the region in which edge effects cannot be ignored.

6

7

8

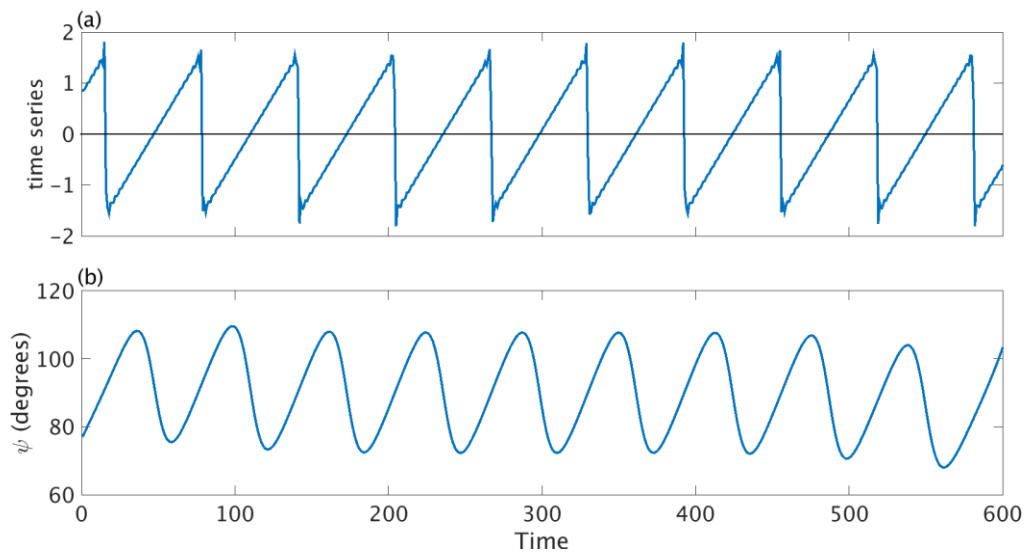


1

2 Figure 2. (a) a skewed time series and (b) its corresponding local biphase. The biphase close to  
3 zero indicates a nonlinear interaction resulting in a skewed oscillation. The biphase was calculated  
4 from the first three cosines in the summation described in the text. The large deviations from zero  
5 at the edges are the result of edge effects.

6

1

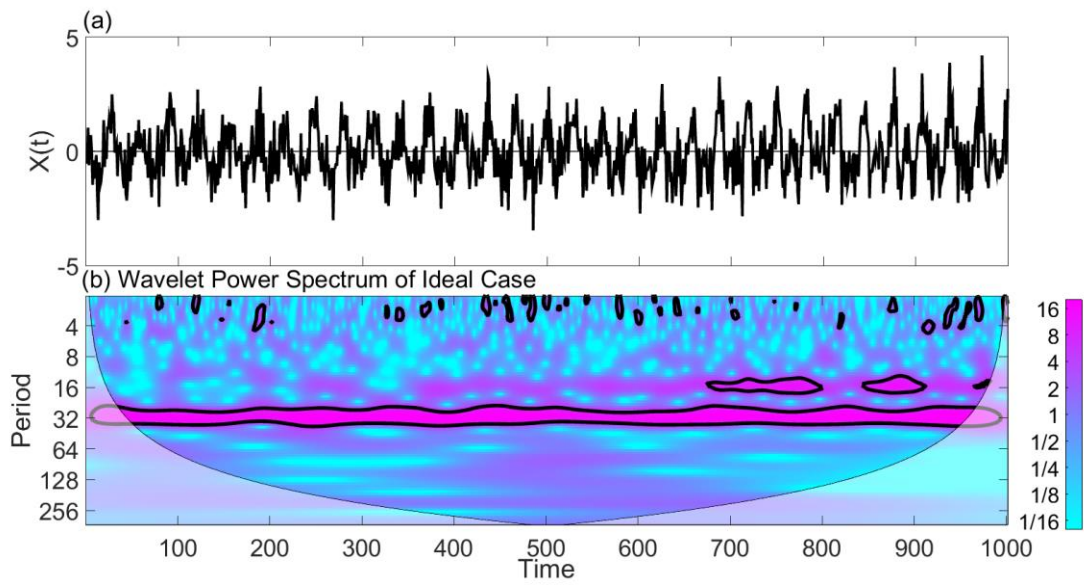


2

3 Figure 3. (a) A saw-toothed time series and (b) its corresponding local biphase. The biphase close  
 4 to  $90^\circ$  indicates a nonlinear interaction resulting in an asymmetric waveform. The biphase was  
 5 calculated from the first three cosines in the summation.

6

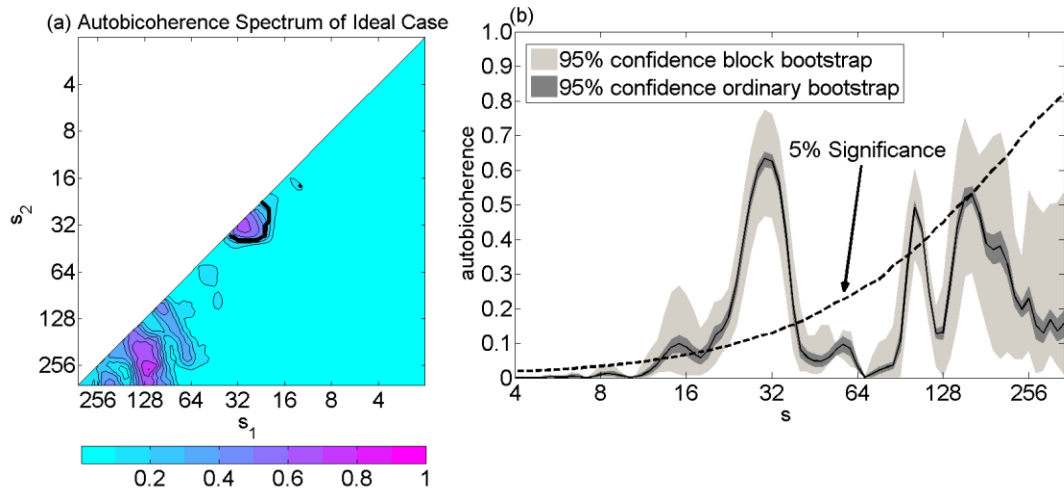
7



1

2 Figure 4. (a) Time series corresponding to Eq. (19). (b) Corresponding wavelet power spectrum.

3

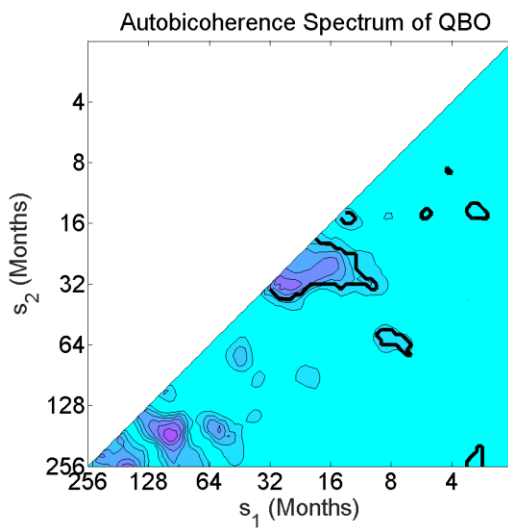


1

2 Figure 5. (a) Wavelet-based autocorrelation spectrum of the ideal time series. Thick contours  
 3 enclose regions of 5% pointwise significance after controlling the FDR. The diagonal line separates  
 4 the spectrum into two symmetric regions. (b) The diagonal slice of the autocorrelation spectrum  
 5 at  $s_1 = s_2 = s$ . The critical level for the test represented by the dotted line was calculated using  
 6 Monte Carlo methods.

7

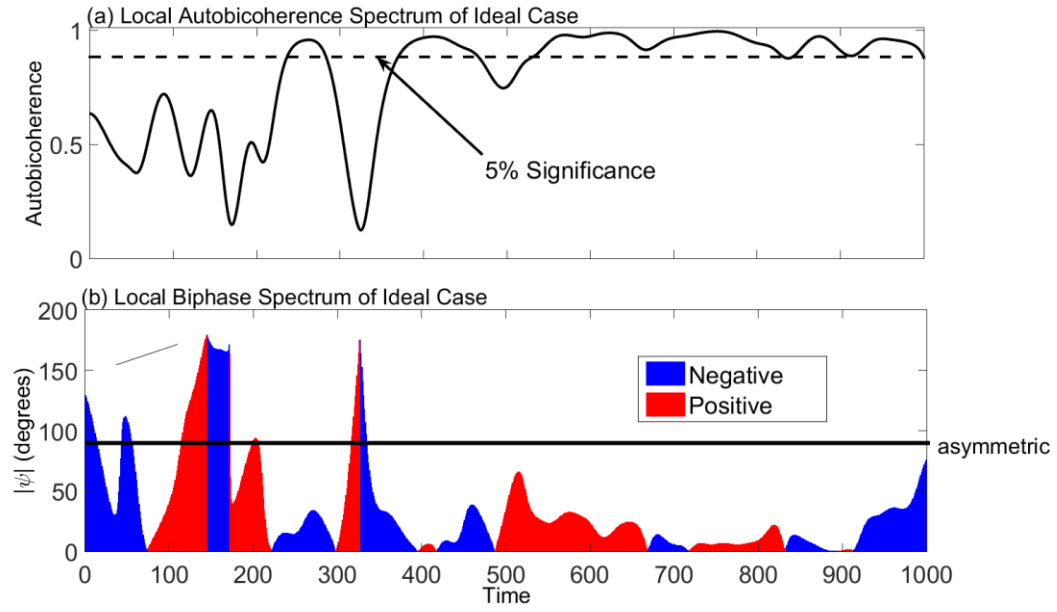
1  
2  
3



5 Figure 6. The wavelet-based autocorrelation spectrum of the QBO index for the period 1950-  
6 2013. Thick contours enclose regions of 5% pointwise significance.

7

8

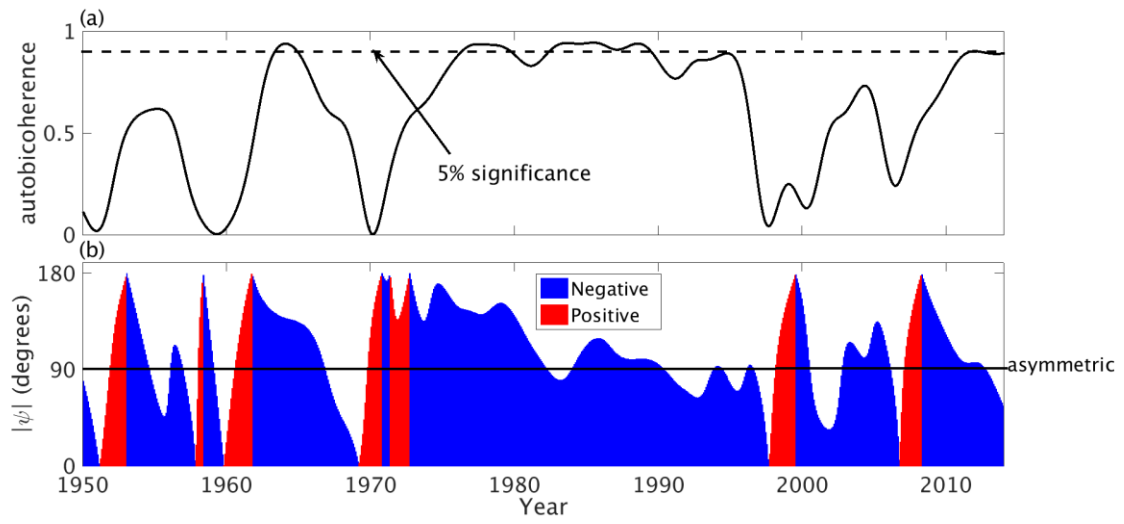


1

2 Figure 7. (a) The local autocohherence and (b) local biphase corresponding to (30, 30) in the full  
 3 autocohherence spectrum shown in Figure 5a. Biphases differing from  $90^\circ$  indicate that the  
 4 nonlinear interaction resulted in a waveform with skewness.

5

6

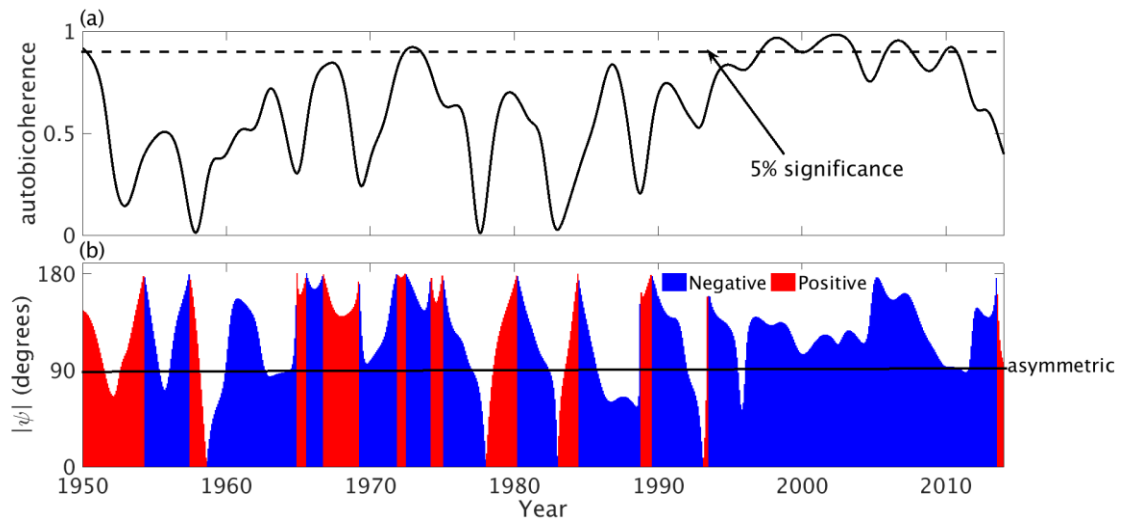


1

2 Figure 8. Same as Fig. 7 except at (28, 28) in the autobicoherence spectrum of the QBO index  
 3 Biphases differing from  $90^\circ$  indicate that the nonlinear interaction resulted in a waveform with  
 4 skewness.

5

1

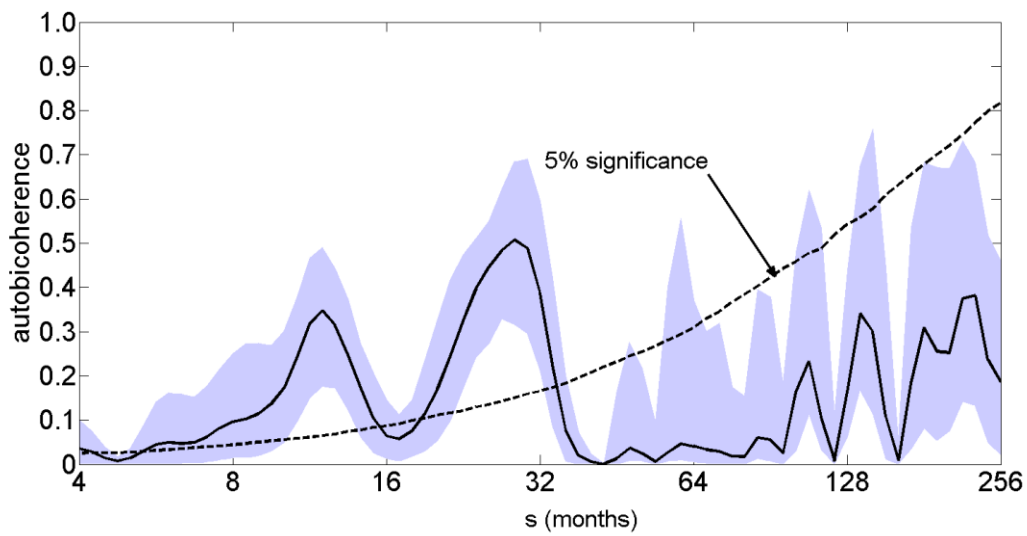


2

3 Figure 9. Same as Fig. 8 except at the point (16, 26).

4

5



- 1
- 2      Figure 10. Same as Fig. 5b except for the QBO index for the period 1950-2013.
- 3
- 4

1    **References**

2    Alley, R. B., Marotzke, J., Nordhaus, W. D., Overpeck, J. T., Peteet, D. M., Pielke Jr., R. A.,  
3    Pierrehumbert, R. T., Rhines, P. B., Stocker, T. F., Talley, L. D., Wallace, J. M.: Abrupt Climate  
4    Change. *Science*, 299, 2005-2010, 2003.

5    Benjamini, Y., Hochberg, Y.: Controlling the False Discovery Rate: A Practical and Powerful  
6    Approach to Multiple Testing. *J. Royal Statistical Society*, 57, 289-300, 1995.

7    Benjamini, Y., Yekutieli, D.: The Control of the False Discovery Rate in Multiple Testing under  
8    Dependency. *Ann Statist.*, 29, 1165-1188, 2001.

9    Collis, W. B., White, P. R. and Hammond, J. K.: Higher-order Spectra: The Bispectrum and  
10   Trispectrum. *Mech. Syst. Signal Process.* 12, 375–394, 1998.

11   Efron, B.: Bootstrap Methods: Another Look at the Jackknife. *Ann. Statist.*, 7, 1–26, 1979.

12   Elgar, S. and Chandran, V.: Higher-order Spectral Analysis to Detect Nonlinear Interactions in  
13   Measured Time Series and an Application to Chua's Circuit. *Internat. J. Bifurcat. Chaos*, 3, 19–  
14   34, 1993.

15   Elgar, S. and Sebert, G.: Statistics of Bicoherence and Biphase. *J. Geophysical Research*, 94,  
16   10993-10998, 1989.

17   Elsayed, M. A. K.: Wavelet Bicoherence Analysis of Wind–wave Interaction. *Ocean Eng.*, 33,  
18   458–470, 2006.

19   Gan, T. Y., Gobena, A. K., and Wang, Q.: Precipitation of Southwestern Canada: Wavelet,  
20   Scaling, Multifractal Analysis, and Teleconnection to Climate Anomalies. *J. Geophys. Res.*, 112,  
21   D10110,

22   Grinsted, A., Moore, J. C. and Jevrejeva, S.: Application of the Cross Wavelet Transform and  
23   Wavelet Coherence to Geophysical Time Series. *Nonlinear Process. Geophys.*, 11, 561–566,  
24   2004.

25   Hagelberg, T., Pisias, N., Elgar, S.: Linear and Nonlinear Couplings between Orbital Forcing and  
26   the Marine  $\delta^{18}\text{O}$  Record during the Late Neocene. *Paleoceanography*, 6, 729–746, 1991.

27   Hamilton, K. and Hsieh, W. W.: Representation of the Quasi-biennial Oscillation in the Tropical  
28   Stratospheric Wind by Nonlinear Principal Component Analysis. *J. Geophys. Res.*, 107, 4232,  
29   doi:10.1029/2001JD001250, 2002.

31   Higuchi, K., Huang, J., Shabbar, A.: A Wavelet Characterization of the North Atlantic Oscillation  
32   Variation and its Relationship to the North Atlantic Sea Surface Temperature. *Int. J. Climatol.*, 19,  
33   1119–1129, 1999.

1

2 Jevrejeva, S., Moore, J. C., Grinsted, A.: Influence of the Arctic Oscillation and El Nino-Southern  
3 Oscillation (ENSO) on Ice Conditions in the Baltic Sea: The wavelet Approach. *J. Geophys. Res.*,  
4 108, 4677, doi:10.1029/2003JD003417, D21, 2003.

5

6 King, T.: Quantifying Nonlinearity and Geometry in Time Series of Climate. *Quat. Sci. Rev.*, 15,  
7 247–266, 1996.

8 Kunsch, H. R.: The Jackknife and the Bootstrap for General Stationary Observations. *Ann. Statist.*,  
9 17, 1217–1241, 1989.

10

11 Labat, D.: Cross Wavelet Analyses of Annual Continental Freshwater Discharge and Selected  
12 Climate Indices. *J. Hydrol.*, 385, 269-278, 2010.

13 Lee, Y. J., Lwiza, K. M.: Factors Driving Bottom Salinity Variability in the Chesapeake Bay. *Cont.*  
14 *Shelf Res.*, 28, 1352-1362, 2008.

15 Lu, B.W., Pandolfo, L., and Hamilton, K.: Nonlinear Representation of the Quasi-Biennial  
16 Oscillation. *J. Atmos. Sci.*, 66, 1886–1904, 2009.

17 Maccarone, T. J.: The Biphase Explained: Understanding the Asymmetries in Coupled Fourier  
18 Components of Astronomical Timeseries, *Mon. Not. R. Astron. Soc.*, 435, 3547, doi:  
19 10.1093/mnras/stu1824, 2013.

20

21 MacDonald, G. M., Case, R. A.: Variations in the Pacific Decadal Oscillation over the Past  
22 Millennium, *Geophys. Res. Lett.*, 32, L08703, doi:10.1029/2005GL022478, 2005.

23

24 Maraun, D., Kurths, J., and Holschneider, M.: Nonstationary Gaussian Processes in the Wavelet  
25 Domain: Synthesis, Estimation, and Significance Testing, *Phys. Rev. E*, 75, doi: 2  
26 10.1103/PhysRevE.75.016707, 2007.

27 Moussas, X., Polygiannakis, J. M., Preka-Papadema, P., Exarhos, G., Solar cycles: A tutorial. *Adv.*  
28 *Sp. Res.*, 35, 725-738, 2005.

29

30 Newman, M., Compo, G. P., Alexander, M. A.: ENSO-forced variability of the Pacific decadal  
31 oscillation. *J. Climate*, 16, 3853-3857, 2003.

32 Nidal, K. and Malik, A. S.: EEG/ERP Analysis: Methods and Applications, CRC Press, 334 pp.,  
33 2013.

34 Nikias, C. L., Raghubeer, M. R.: Bispectrum Estimation: A Digital Signal Processing Framework,  
35 IEEE, 75, 869-891, 1987.

36 Olsen, J., Anderson, J. N., Knudsen, M. F.: Variability of the North Atlantic Oscillation over the  
37 past 5,200 years, *Nature Geosci.*, 5, 808-812, 2012.

1 Polygiannakis, J. M., Moussas, X., Sonett, C. P. A Nonlinear RLC Solar Cycle Model. *Sol. Phys.*  
2 163, 193–203, 1996.

3 Polygiannakis, J., Preka-Papadema, P., Moussas, X.: On Signal–noise Decomposition of Time-  
4 series using the Continuous Wavelet Transform: Application to Sunspot Index. *MNRAS*, 343, 725-  
5 734, 2003.

6

7 Rial, J. A., Anacleto, C. A.: Understanding Nonlinear Responses of the Climate System  
8 to Orbital Forcing. *Quat. Sci. Rev.*, 19, 1709-1722, 2000.

9

10 Rusu, M. V.: The Asymmetry of the Solar Cycle: A result of Non-linearity, *Adv. Sp. Res.*, 40,  
11 1904-1911, 2007.

12 Rutherford, S., D'Hondt, S.: Early Onset and Tropical Forcing of 100,000-year Pleistocene Glacial  
13 Cycles. *Nature*, 408, 72-75, 2000.

14

15 Schulte, J. A., Duffy, C., and Najjar, R. G.: Geometric and Topological Approaches to Significance  
16 Testing in Wavelet Analysis. *Nonlin. Processes Geophys.*, 22, 139-156, 2015.

17 Schulte, J. A., Najjar, R. G., Lee, S.: Salinity and Streamflow Variability in the Mid-Atlantic  
18 Region of the United States and its Relationship with Large-scale Atmospheric Circulation  
19 Patterns, *J. Hydrology*, submitted.

20

21 Schulte, J. A.: Cumulative areawise testing in wavelet analysis and its application to geophysical  
22 time series, *Nonlin. Processes Geophys.*, 23, 45-57, doi:10.5194/npg-23-45-2016, 2016.

23

24 Timmermann A.: Decadal ENSO Amplitude Modulations: a Nonlinear Paradigm. *Global Planet  
25 Change*, 37, 135-156, 2003.

26

27 Torrence, C. and Compo, G. P.: A Practical Guide to Wavelet Analysis, *Bull. Am. Meteorol. Soc.*,  
27 79, 61–78, 1998.

28

29 Torrence, C., Webster, P. J.: Interdecadal Changes in the ENSO–Monsoon System. *J. Climate*, 12,  
29 2679–2690, 1999.

30

31 Van Milligen, B. P., Sánchez, E., Estrada, T., Hidalgo, C., Brañas, B., Carreras, B., García, L.:  
Wavelet Bicoherence: A New Turbulence Analysis Tool. *Phys. Plasmas*, 2, 3017-3032, 1995.

32

33 Velasco, V. M. and Mendoza, B.: Assessing the Relationship between Solar Activity and Some  
Large Scale Climatic Phenomena, *Adv. Sp. Res.*, 42, 866–878, 2008.

34

35 Watson, P. A. G. and Gray, L. J.: How Does the Quasi-Biennial Oscillation Affect the  
Stratospheric Polar Vortex?. *J. Atmos. Sci.*, 71, 391–409, 2014.

36 Wilks, D. S.: Resampling Hypothesis Tests for Autocorrelated Fields. *J. Clim.*, 10, 65–82, 1997.

1

2

3

4